Learning a spatio-temporal latent atlas for fetal brain segmentation

Eva Dittrich[1⋆], Tammy Riklin-Raviv[2], Gregor Kasprian[3], Peter C. Brugger[4], Daniela Prayer[3], and Georg Langs[1,5]

[1] Computational Image Analysis and Radiology Lab, Department of Radiology, Medical University of Vienna, Austria, eva.dittrich@meduniwien.ac.at,
[2] SPL, Brigham and Women's Hospital, Harvard Medical School, Boston, USA
[3] Department of Radiology, Medical University of Vienna, Vienna, Austria
[4] Department of Systematic Anatomy, Medical University of Vienna, Vienna, Austria
[5] CSAIL, Massachusetts Institute of Technology, Cambridge, MA, USA

Abstract. Fetal Magnetic Resonance Imaging (MRI) in early phases of the cerebral development during gestation offers insights into the emergence of brain structures, their characteristics and variability across the population. To collect substantial bodies of observations automatic analysis of these data is necessary. However, automatic segmentation proofs challenging due to image quality, low contrast between brain tissues, and the rapid development at this early age. Current atlas-based segmentation approaches perform well in the adult population, but they are unable to cover the rapid changes during early development phases. In this paper, we introduce a spatio-temporal group-wise segmentation of fetal brain structures given a single annotated example. The method is based on an emerging spatio-temporal latent atlas that captures the age-dependent characteristics in the training population, and supports the segmentation of brain structures. The proposed atlas makes segmentation of subcortical structures possible by integrating information across a large number of subjects. It encodes the average development and its variability, which is ultimately relevant for diagnosis. Furthermore, we introduce a method to re-estimate each subject's age to accommodate variability in developmental speed. Results on 33 cases from 20th to 30th gestational week demonstrate improved segmentation results, and an estimate of average development.

Keywords: Atlas building, Fetal brain development, Segmentation

1 Introduction

Novel imaging methods, such as ultra-fast Magnetic Resonance Imaging (MRI), allow for high-resolution image acquisition in utero [7, 12]. Fig. 1 shows fetal brains at the age of 20, 25 and 30 gestational weeks (GW). Despite the wealth of information these data provide, currently, the assessment is typically performed

⋆ E. Dittrich is a recipient of a DOC-fFORTE-fellowship of the Austrian Academy of Sciences. This work was partly funded by The European Union (257528, KHRES-MOI), and the Austrian Sciences Fund (P 22578-B19, PULMARCH).

Fig. 1. Example slices of fetal brain volumes showing the development at GW 20, 25 and 30.

qualitatively. Clinicians and researchers lack a quantitative reference that captures the developmental characteristics, and variability in the population. A key to this understanding is to learn spatio-temporal models, and corresponding segmentations of the brain structures in this period from in vivo data.

Atlases exist for the adult [4–6] or neonatal brain [1, 9, 11]. However, no comprehensive quantitative atlas of fetal development is available. A major challenge is the rapid and substantial change the brain undergoes during this period. It makes the temporal component a crucial part of any modeling approach, and limits the applicability of standard methods such as group-wise registration [4, 6]. At the same time, a large number of cases is necessary to learn a representative model of the developmental variability. A promising related result was reported in [8]. However, this method requires a manual annotation for all data.

In this work, we propose a method for the building of a *spatio-temporal latent atlas* from a single annotated example and a large number of non-annotated examples. The atlas captures the development and variability of a cerebral structure in healthy fetal brains during the gestational age of 20-30 weeks. It can serve as a reference map to represent the sequence of individual developmental stages, or to compare individual cases to control population statistics. The present work is closely related to the latent atlas proposed in [13]. It advances the approach presented in [13] by two essential aspects: **1.** it tackles the question of fetal brain development by incorporating a time component, and is thereby able to cope with the substantial changes of fetal brain structures parameterized by the gestational age. **2.** It provides an important clinical benefit by enabling an estimation of a subject's gestational age based on correlation with the cohort. This takes into account that not all fetuses grow exactly as expected by common literature [7]. In case the development is behind or ahead of its expected time, it is possible to confuse these minor age changes with severe diseases (i.e. lissencephaly, a form of malformation of cortical diseases). The age re-estimation presented above respects the possibility of a small age shift and corrects for it.

2 Learning a spatio-temporal latent atlas from partially annotated data

This section introduces the spatio-temporal atlas and its construction having individual training images. The atlas as well as the segmentations of the MR images are obtained via an iterative optimization process given a unified cost functional that incorporates both spatial and temporal components. The pro-

posed method also allows a fine tuning of the subjects gestational age as an inherent part of the entire optimization procedure.

Our objective is to segment a specific subcortical structure from N fetal MR images. Each of the images $\mathbf{I}_n : \Omega \rightarrow \mathbf{R}^+$ $(n = 1, ..., N)$ has $\mathbf{v}$ voxels defined on $\Omega \subset \mathbf{R}^3$. We denote by $\Gamma_n : \Omega \rightarrow \{0, 1\}$ the segmentation of image I_n. Furthermore, each image is assigned to a nominal age $\mu(n) \in \{\tau_1 \dots \tau_K\}$ measured in weeks. We make the assumption that Γ_n induces the image $\mathbf{I}_n$ with probability $p(\mathbf{I}_n|\Gamma_n; \theta_{\mathbf{I},n})$, independently from all other pairs of images and segmentations. We model the intensity distribution with a Gaussian mixture model (GMM). We denote by $\theta_{\mathbf{I},n}$ the GMM parameters corresponding to the intensity distribution of an image $\mathbf{I}_n$. We also assume that the segmentations are drawn I.I.D. from a probability distribution $p(\Gamma; \theta^{\mu}_{\Gamma})$, with $\theta^{\mu}_{\Gamma} : \Omega \rightarrow [0, 1]$ being the latent spatio-temporal model parameters. As we will show in the following, this definition of latent parameters extends [13] due to the temporal dependency.

2.1 Cost functional

We use a probabilistic level-set formulation to segment an ensemble of aligned images and to construct a probabilistic spatio-temporal atlas. Let $\phi_n : \Omega \rightarrow \mathbf{R}$ denote a level-set function that defines the binary segmentation Γ_n of an image $\mathbf{I}_n$, such that its zero-level $\partial\phi_n$ represents the boundary of the structure of interest. As in [2] we use a smooth approximation of the Heaviside function $\tilde{H}(\phi_n)$ to partition the image domain Ω into foreground and background regions. The formulations we use for $\tilde{H}(\phi)$ and its derivative with respect to ϕ, i.e. $\tilde{\delta}(\phi)$ are the same as in [13]. We next construct a unified cost functional of $\{\phi_n\}$. The joint estimation of the unknown model parameters $\Theta = \{\theta_{\Gamma}, \theta_{\mathbf{I},1}, ..., \theta_{\mathbf{I},N}\}$ and the segmentations Γ_n (or ϕ_n) is obtained by an alternating minimization process of the cost functional using calculus of variations. The proposed cost functional $C(\phi_1, \dots, \phi_n, \Theta)$ is the weighted sum of several energy terms:

$$C(\phi_1, \dots, \phi_n, \Theta) = \gamma C_L + \beta C_I + \alpha C_S + \eta C_A \tag{1}$$

where C_L is the classic smoothness term, C_I is an image likelihood term, C_S is a spatial term, C_A is an area term and $\alpha, \beta, \gamma, \eta$ are the corresponding weight parameters. The mathematical formulation of these terms is given as follows:

Spatio-temporal term: This term is the main innovative component of the proposed framework. It links the segmentations of the training images and the spatio-temporal atlas, and is a function of the latent model parameters θ^{μ}_{Γ}, i.e. the spatial parameters corresponding to gestational age μ (details in Sec. 2.3):

$$C_S(\phi_n, \Theta) = -\int_{\Omega} [\tilde{H}(\phi_n(\mathbf{x})) \log \theta^{\mu}_{\Gamma}(\mathbf{x}) + \tilde{H}(-\phi_n(\mathbf{x})) \log(1 - \theta^{\mu}_{\Gamma}(\mathbf{x}))] d\mathbf{x} \tag{2}$$

Image likelihood term: Let p_{in} and p_{out} define the intensity distribution of the foreground and the background regions, correspondingly. Since we deal with MR images that contain multiple tissue classes we chose a mixture of Gaussians to represent the background intensity distribution. In our experiments two Gaussians proved sufficient. We assume normal distribution of the structure of interest's intensities. We use an image likelihood term as derived in [13]:

$$C_I(\phi_n, \Theta) = -\int_\Omega [\tilde{H}(\phi_n(\mathbf{x}))\log(p_{in}(\mathbf{I}_n;\theta_{\mathbf{I},n}))+\tilde{H}(-\phi_n(\mathbf{x}))\log(p_{out}(\mathbf{I}_n;\theta_{\mathbf{I},n}))]d\mathbf{x}. \tag{3}$$

Length term: C_L denotes the **contour length regularizer**. It is commonly used in the level-set literature (like [2]), controls the length of the segmentation, and restrains boundary smoothness.

$$C_L(\phi_n) = \int_\Omega |\nabla \tilde{H}(\phi_n(\mathbf{x}))|d\mathbf{x} \tag{4}$$

Area term. The **area term** (with similar behavior as a balloon force [3]) is denoted by C_A, and describes the area of the shape or structure of interest.

$$C_A(\phi_n) = \int_\Omega \tilde{H}(\phi_n(\mathbf{x}))d\mathbf{x} \tag{5}$$

2.2 Optimization of the cost functional

The cost function (Eq. 1) is optimized by applying two steps in an alternating manner: for fixed model parameters $\mathbf{\Theta}$, the level set function ϕ_n is evolved by the following gradient descent equation:

$$\phi_n(\mathbf{x}, t + \Delta t) = \phi_n(\mathbf{x}, t) + \Delta t \frac{\partial \phi_n}{\partial t} \tag{6}$$

where t represents the time parameter, and Δt controls the update step width. $\frac{\delta \phi_n}{\delta t}$ is computed using the Euler-Lagrange equations, leading to:

$$\frac{\partial \phi_n}{\partial t} = \delta(\phi_n)\{\gamma \text{ div } (\frac{\nabla \phi_n}{|\nabla \phi_n|}) + \beta[\log p_{in}(\mathbf{I}_n(\mathbf{x});\theta_{\mathbf{I},n}) - \tag{7}$$

$$- \log p_{out}(\mathbf{I}_n(\mathbf{x});\theta_{\mathbf{I},n})] + \alpha[\log \theta_\Gamma - \log(1-\theta_\Gamma)] + \eta\} \tag{8}$$

Then, we fix the segmentations ϕ_n and update the model parameters (intensity and spatial parameters) by computing derivatives of the cost function in Eq. 1 with respect to each parameter. The spatial function θ_Γ^μ is unique to each subject's age. It is estimated by optimizing the sum of cost terms dependig on θ_Γ^μ:

$$\theta_\Gamma^\mu \approx \arg\max \sum_{n=1}^{N} \int_\Omega [\tilde{H}(\phi_n(\mathbf{x}))\log(\theta_\Gamma^\mu(\mathbf{x})) + (1-\tilde{H}(\phi_n(\mathbf{x})))\log(1-\theta_\Gamma^\mu(\mathbf{x}))]d\mathbf{x}, \tag{9}$$

resulting in the spatio-temporal atlas function in Eq. 10.

2.3 A spatio-temporal template

The atlas links the segmentations in all training images. However, it is not a single probabilistic template, but depends on the gestational age μ of the training example it is applied to. Thus, instead of averaging over the segmentation probability maps of all the subjects (as performed in [13]), we introduce a weighted sum, with weights $w_{\mu,\mu(n)}$ that balance the influence of segmentations in examples with different ages. This is similar in spirit to kernel-based registration techniques such as [4]. The weighting is central to incorporate the spatio-temporal

characteristics into the atlas. The weights are established to fulfill the following constraints: Consider two images $\mathbf{I}_k$ and $\mathbf{I}_j$ with gestational ages $\mu(k)$, and $\mu(j)$ respectively ($j, k \in \{1, ..., N\}$). $\Delta\mu_{k,j} = \mu(k) - \mu(j)$ denotes the age difference between these images. If $\Delta\mu_{k,j} = 0$, i.e. the subjects have the same gestational age then the segmentation Γ_j has the largest influence on $\theta_\Gamma^{\mu(k)}$ and vice versa. That is, subjects of the same age share the same atlas ($\Delta\mu_{k,j} = 0$) $\Rightarrow$ ($\theta_\Gamma^{\mu(k)} = \theta_\Gamma^{\mu(j)}$), therefore the atlas is age-dependant rather than subject-identity dependent. Let σ define the age range that should be considered for the age-dependent atlas generation. For $\sigma << 1$, only segmentation of subjects of similar ages are considered in the atlas computation. When $\sigma \to \infty$, the segmentations are equally weighted as in the original latent atlas framework. Our spatio-temporal latent atlas for all subjects of age μ is defined as follows:

$$\theta_\Gamma^\mu(\mathbf{x}) = \frac{1}{W_\mu} \sum_{n=1}^{N} w_{\mu,\mu(n)} \tilde{H}(\phi_n(\mathbf{x})), \text{ where } w_{\mu,\mu(n)} = e^{-\frac{(\mu-\mu(n))^2}{\sigma^2}} \tag{10}$$

with $W_\mu = \sum_{n=1}^{N} w_{\mu,\mu(n)}$ as normalization term.

2.4 Age re-estimation

While learning the atlas, we can re-estimate the subject's age based on the segmented structure, and its similarity to other cases in the training population. For this, we compose an energy function

$$\xi = \sum_m \sum_n \omega_{\mu(m),\mu(n)} (\Gamma_m \log \Gamma_n + (1 - \Gamma_m) \log(1 - \Gamma_n)). \tag{11}$$

The minimum of this energy function reveals the subject's estimated age, i.e. the age based upon which the subject best fits to the cohort. Thus, for a large ξ, the segmented structures Γ_m and Γ_n differ from each other, resulting in a dissimilar age. In contrast to this, if ξ is small, the structures are approximately the same age. The age *correction* can further be seen as an extraction of information about how the age indicated by the state of morphological development deviates from the nominal age.

2.5 Preprocessing

The proposed method is based on a preliminary registration of all volumes. We use a surface-based spatio-temporal group-wise registration [10] to achieve an initial positioning. Based on the alignment of surface points, the brain volume is registered. In addition, we perform a local refinement during the iterative optimization process. Each image is translated to the point of highest correlation with the probabilistic atlas θ_Γ^μ. In a coarse initialization, the segmentation Γ_k of a reference image $\mathbf{I}_k$ (with $k \in \{1, ..., N\}$) is mapped onto all images. The goal is to estimate the remaining segmentations Γ_n ($n \in \{1, ..., N\} \setminus \{k\}$). Since the model parameters are also unknown, we now alternate between estimating segmentations $\mathbf{\Gamma}$ and refining model parameters $\mathbf{\Theta}$ [13].

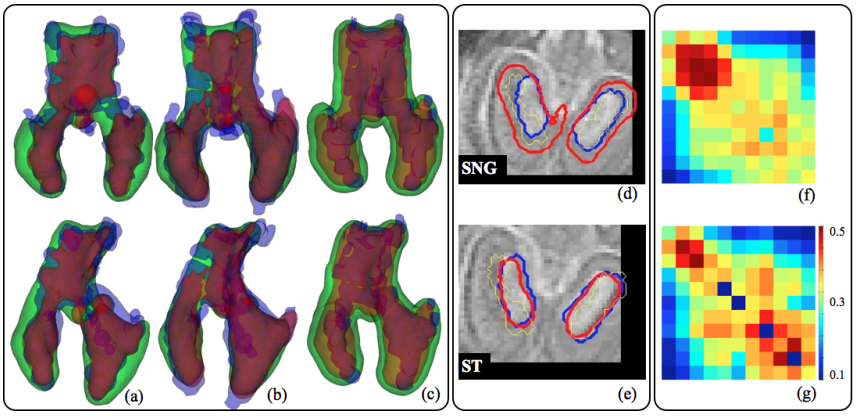

Fig. 2. (a-c): 3D visualization (with 2 different views each) of segmentation results (red) compared to the ground truth (blue) and the resulting atlas (green) for subjects at (a) 21, (b) 23, (c) 26 GWs. Obviously, there is a high overlap of the segmentation and the ground truth, and the segmentation shows a more natural shape of the ventricle than its serrated annotation. (d-e): Segmentation accuracy of the SNG atlas (d), and our improved ST atlas (e) for a fetus at 21 GW after 50 iterations (yellow = initialization, blue = ground truth, red = segmentation result). Dice score of the ground truth before (f), and after the age optimization (g).

3 Data

This project is an ongoing collaboration with neuroradiologists and anatomists specialized on fetal MRIs. We evaluated our approach on 33 coronal in utero MR scans depicting healthy fetal brains from GW 20 to 30. We excluded cases suspicious for cardiac abnormalities, complex syndromes or chromosomal abnormalities. Data (T2-weighted MRI) was acquired by a single-shot, fast spin-echo 1.5 Tesla Philips Gyroscan during clinical routine with in-plane resolution 0.78-0.9 pixels/mm, slice thickness 3-4.4mm, image resolution 256×256, FOV $200mm$, SAR $< 9\%/0.4$ W/kg, image acquisition time $\leq 20s$, TE 100-140ms, TR 14000ms. During image acquisition, neither the fetus nor the mother were sedated. We chose a larger slice thickness to avoid motion artifacts, and included only cases where the degree of fetal motion was acceptable. Isotropic resolution was gained by cubic data interpolation. To obtain a standard of reference for validation, a medical expert manually segmented the ventricles in each of these images.

4 Results and Discussion

The parameter settings were selected based on cross validation, resulting in a constellation of $\alpha = 0.1, \beta = 0.1, \gamma = 0.3, \eta = 0.6$ for the cost term weights, and $\sigma = 2$ for the spatio-temporal age weight. 2 Gaussians were used to model the background intensity distribution, the remaining GMM parameters were established by expectation maximization (EM). As reference, we selected a fetal brain at 24 GWs since at this age the subcortical structures are best perceptible (according to the collaborating anatomist).

We compared the proposed spatio-temporal latent atlas (ST) to the latent atlas presented in [13] (denoted by *single (or SNG) atlas*). Each image's segmentation by the ST atlas is evaluated with respect to the ground truth, and compared to the accuracy achieved by the SNG atlas. A comparison of the segmentation result (after 50 iterations) for a fetal brain at 21 GW is given in Fig. 2(d-e). The update of the segmentation, and its convergence towards the ground truth is visible: the current segmentation (red) is translated in the direction of the actual ground truth (blue), even though it was initialized at the yellow area. Starting from a mean/median Dice score of 0.44/0.47 after the first iteration, the SNG atlas dropped to 0.36/0.35, whereas the proposed ST atlas achieved a mean/median Dice score of 0.61/0.60. This difference indicates clearly that the temporal component in the ST atlas improves segmentation accuracy while a single SNG template is not sufficient for joint segmentation. After visual inspection of segmentation result and annotation (see Fig. 2(a-c)), we attribute the still relatively low ST Dice score to yet imperfect serrated annotations and potentially minimal remaining motion artifacts.

To validate the developmental age estimation method, we conducted an experiment where 11 manual annotations were used to perform the age optimization. Fig. 2(f-g) shows a joint histogram of the pairwise Dice scores between all cases of different gestational age before (f) and after (g) age optimization.[1] Consistent with the expectation, the histogram becomes narrower after the optimization. The age correction improves the coherence of the data, and is able to explain a part of the shape variability by a shift in age.

5 Conclusion

We propose a probabilistic spatio-temporal latent atlas for the segmentation of cerebral structures during early brain development. From a single annotated example and a set of images without annotation we learn an atlas and segmentations of an anatomical structure. The images are samples of a developmental process and the spatio-temporal latent atlas is a continuous distribution of average templates for each age in the observed interval. Experiments show that the proposed spatio-temporal latent atlas outperforms an existing atlas approach without age specificity by learning time dependent shape of the structure during segmentation. Although the segmentation accuracy improves, we expect further improvement by including a larger training sample, and more accurate non-rigid registration. The benefits of the atlas are two-fold. First, it serves as a prior during segmentation of large numbers of examples for structures that undergo development, and secondly, the atlas itself is informative regarding the underlying developmental process. Finally, we show that gestational age estimation can partially explain shape variability by age shifts, which is highly relevant in a clinical context where the developmental process and possible pathological deviations have to be assessed. There are several interesting questions future work

[1] Note that we excluded the computation of the Dice score between each case and itself. Thus, if there is only one case in a specific week, its entry in the diagonal of the matrix is of course zero.

will focus on. In the context of age estimation, we have to better understand how to reliably attribute variability to anatomical variability, or differences in developmental speed. Furthermore, the inclusion of multiple subcortical structures in the atlas building and segmentation process is a natural next step. Lastly, the choice of reference examples can have an influence on the segmentation, but since after initialization all images are treated equally, this influence is relatively small during optimization. Thus, the possible inclusion of multiple annotated examples is a straightforward extension of the proposed framework.

References

1. Aljabar, P., Wolz, R., Srinivasan, L., Counsell, S., Boardman, J., Murgasova, M., Doria, V., Rutherford, M., Edwards, A., Hajnal, J.: Combining Morphological Information in a Manifold Learning Framework: Application to Neonatal MRI. Medical Image Computing and Computer-Assisted Intervention 6363(3), 1–8 (2010)
2. Chan, T., Vese, L.: Active contours without edges. IEEE Transactions on Image Processing 10(2), 266–277 (2001)
3. Cohen, L., Cohen, I.: Finite-element methods for active contour models and balloons for 2-D and 3-D images. Pattern Analysis and Machine Intelligence 15(11), 1131–1147 (1993)
4. Davis, B., Fletcher, P., Bullitt, E., Joshi, S.: Population shape regression from random design data. ICCV 10, 1–7 (2007)
5. Ericsson, A., Aljabar, P., Rueckert, D.: Construction of a patient-specific atlas of the brain: Application to normal aging. IEEE International Symposium on Biomedical Imaging pp. 480–483 (2008)
6. Fischl, B., Salat, D., van der Kouwe, A., Makris, N., Ségonne, F., Quinn, B., Dale, A.: Sequence-independent segmentation of magnetic resonance images. Neuroimage 23, S69–S84 (2004)
7. Garel, C.: MRI of the Fetal Brain: Normal Development and Cerebral Pathologies, vol. 1. Springer (2004)
8. Habas, P.A., Kim, K., Corbett-Detig, J.M., Rousseau, F., Glenn, O.A., Barkovich, A.J., Studholme, C.: A spatiotemporal atlas of MR intensity, tissue probability and shape of the fetal brain with application to segmentation. NeuroImage pp. 1–35 (Jun 2010)
9. Kuklisova-Murgasova, M., Aljabar, P., Srinivasan, L., Counsell, S., Doria, V., Sera, A., Gousias, I., Boardman, J., Rutherford, M., Edwards, D., Hajnal, J., Rueckert, D.: A dynamic 4D probabilistic atlas of the developing brain. NeuroImage (Jan 2010)
10. Langs, G., Kasprian, G., Dittrich, E., Bittner, M., Brugger, P., Prayer, D.: Groupwise spatio-temporal registration and segmentation of fetal cortical surface development. MICCAI 2010 Workshop STIA'10 pp. 1–12 (Aug 2010)
11. Murgasova, M., Dyet, L., Edwards, D., Rutherford, M., Hajnal, J., Rueckert, D.: Segmentation of brain MRI in young children. Academic radiology 14(11), 1350–1366 (2007)
12. Prayer, D., Kasprian, G., Krampl, E., Ulm, B., Witzani, L., Prayer, L., Brugger, P.: MRI of normal fetal brain development. European Journal of Radiology 57, 199–216 (2006)
13. Riklin-Raviv, T., Van Leemput, K., Menze, B., Wells III, W., Golland, P.: Segmentation of Image Ensembles via Latent Atlases. Medical Image Analysis 14, 654–665 (2010)